



## Modification of the Antibiotic, Colistin, with Dextrin Causes Enhanced Cytotoxicity and Triggers Apoptosis in Myeloid Leukemia

Siân Rizzo, Mathieu Varache, Edward J Sayers, Arwyn T Jones, Alex Tonks, David W Thomas & Elaine L Ferguson

To cite this article: Siân Rizzo, Mathieu Varache, Edward J Sayers, Arwyn T Jones, Alex Tonks, David W Thomas & Elaine L Ferguson (2024) Modification of the Antibiotic, Colistin, with Dextrin Causes Enhanced Cytotoxicity and Triggers Apoptosis in Myeloid Leukemia, International Journal of Nanomedicine, , 5419-5437, DOI: [10.2147/IJN.S449185](https://doi.org/10.2147/IJN.S449185)

To link to this article: <https://doi.org/10.2147/IJN.S449185>



© 2024 Rizzo et al.



Published online: 07 Jun 2024.



Submit your article to this journal [↗](#)



Article views: 3






View related articles [↗](#)



View Crossmark data [↗](#)

# Modification of the Antibiotic, Colistin, with Dextrin Causes Enhanced Cytotoxicity and Triggers Apoptosis in Myeloid Leukemia

Siân Rizzo <sup>1</sup>, Mathieu Varache <sup>1</sup>, Edward J Sayers <sup>2</sup>, Arwyn T Jones<sup>2</sup>, Alex Tonks <sup>3</sup>, David W Thomas<sup>1</sup>, Elaine L Ferguson <sup>1</sup>

<sup>1</sup>Advanced Therapies Group, School of Dentistry, Cardiff University, Cardiff, UK; <sup>2</sup>School of Pharmacy and Pharmaceutical Sciences, Cardiff University, Cardiff, UK; <sup>3</sup>Department of Haematology, School of Medicine, Cardiff University, Cardiff, UK

Correspondence: Elaine L Ferguson, Advanced Therapies Group, School of Dentistry, Cardiff University, Cardiff, UK, Tel +44 2922 510663, Email FergusonEL@cardiff.ac.uk

**Introduction:** Acute myeloid leukemia (AML) remains difficult to treat due to its heterogeneity in molecular landscape, epigenetics and cell signaling alterations. Precision medicine is a major goal in AML therapy towards developing agents that can be used to treat patients with different ‘subtypes’ in combination with current chemotherapies. We have previously developed dextrin–colistin conjugates to combat the rise in multi-drug resistant bacterial infections and overcome dose-limiting nephrotoxicity. Recent evidence of colistin’s anticancer activity, mediated through inhibition of intracellular lysine-specific histone demethylase 1 (LSD1/KDM1A), suggests that dextrin–colistin conjugates could be used to treat cancer cells, including AML. This study aimed to evaluate whether dextrin conjugation (which reduces in vivo toxicity and prolongs plasma half-life) could enhance colistin’s cytotoxic effects in myeloid leukemia cell lines and compare the intracellular uptake and localization of the free and conjugated antibiotic.

**Results:** Our results identified a conjugate (containing 8000 g/mol dextrin with 1 mol% succinylation) that caused significantly increased toxicity in myeloid leukemia cells, compared to free colistin. Dextrin conjugation altered the mechanism of cell death by colistin, from necrosis to caspase 3/7-dependent apoptosis. In contrast, conjugation via a reversible ester linker, instead of an amide, had no effect on the mechanism of the colistin-induced cell death. Live cell confocal microscopy of fluorescently labelled compounds showed both free and dextrin-conjugated colistins were endocytosed and co-localized in lysosomes, and increasing the degree of modification by succinylation of dextrin significantly reduced colistin internalization.

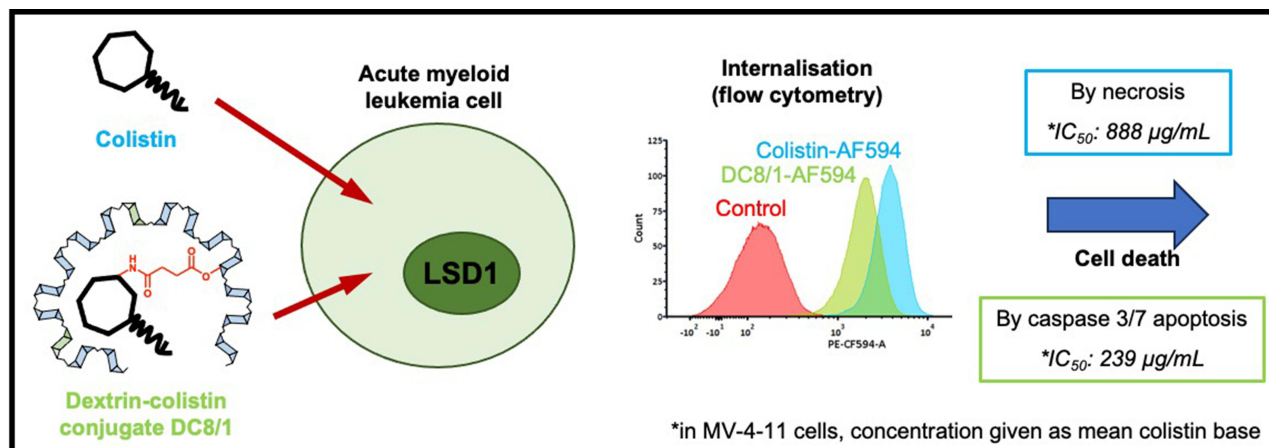
**Discussion:** Whilst clinical translation of dextrin–colistin conjugates for the treatment of AML is unlikely due to the potential to promote antimicrobial resistance (AMR) and the relatively high colistin concentrations required for anticancer activity, the ability to potentiate the effectiveness of an anticancer drug by polymer conjugation, while reducing side effects and improving biodistribution of the drug, is very attractive, and this approach warrants further investigation.

**Keywords:** polymer therapeutics, biodegradable, internalization, polysaccharide, antibiotic

## Introduction

Acute myeloid leukemia (AML) is characterized by a block in hematopoietic differentiation where the hematopoietic stem cell (HSC) fails to develop into mature myeloid cells resulting in bone marrow failure.<sup>1</sup> AML arises due to a wide range of molecular abnormalities and genetic mutations, making the disease difficult to treat.<sup>2</sup> Although AML accounts for fewer than 1% of all new cancer cases,<sup>3</sup> recurrence after complete remission is common. Importantly, infection, due to treatment-related immunosuppression, expression of immunosuppressive molecules or specific defects in the immune response, remains a major cause of death in patients with AML, requiring antibacterial or antiviral therapies to treat infections during first-line treatment.<sup>4</sup> Given the high costs, high risk of failure and protracted development times of new chemotherapy drugs, exploiting the off-target effects of existing antimicrobial agents is an attractive approach to improve survival rates in cancer patients.

## Graphical Abstract



Polymer therapeutics are an important class of drugs that use conjugation of water-soluble polymers to improve the therapeutic index of drugs, including for oncology. Oncaspar<sup>®</sup>, a PEG-L-asparaginase conjugate, was one of the first polymer therapeutics to receive FDA approval, for the treatment of acute lymphoblastic leukemia (ALL).<sup>5</sup> There are currently several nanomedicines in clinical use or undergoing clinical trials for the treatment of AML, including liposomes (eg, VYXEOS<sup>®</sup>; liposomal daunorubicin and cytarabine),<sup>6</sup> polymeric nanoparticles (eg, AZD2811; aurora kinase B inhibitor-loaded Accurin<sup>TM</sup> polymeric nanoparticles)<sup>7</sup> and polymer-drug conjugates (eg, N-(2-hydroxypropyl) methacrylamide (HPMA) copolymer-cytarabine and GDC-0980 conjugates).<sup>8</sup> We have previously developed bio-triggered polymer therapeutics, based on the attachment of the polysaccharide, dextrin, to a bioactive molecule, including phospholipase A2 (PLA2),<sup>9</sup> epidermal growth factor<sup>10</sup> and colistin (also known as polymyxin E),<sup>11</sup> as treatments for breast cancer, chronic wounds and bacterial infection, respectively. Dextrin is an attractive polymeric carrier for protein and peptide drugs as it is non-toxic, non-immunogenic and biodegradable. Varying dextrin's molecular weight and degree of modification by succinylation can control the rate of amylase-mediated degradation, and hence payload release rate.<sup>12–14</sup>

Recently, it has been shown that the polymyxin antibiotics, polymyxin B and colistin, can kill some types of cancer cells,<sup>15</sup> including the ALL cell line REH.<sup>16</sup> Polymyxin's anticancer activity is believed to be mediated through inhibition of lysine-specific histone demethylase 1 (LSD1, also referred to as lysine-specific demethylase 1A: KDM1A),<sup>17</sup> a nuclear histone-modifying enzyme which is overexpressed in AML leading to poorer clinical outcomes.<sup>18</sup> Recently, it has been shown that inhibition of LSD1/KDM1A activity results in inhibition of AML cell proliferation and enhanced differentiation.<sup>18</sup> Thus, several LSD1/KDM1A inhibitors, including GSK2879552 and tranlycypromine, are currently in clinical trials for cancer treatment,<sup>19</sup> including AML, as a combination therapy.<sup>20</sup> Given the efficacy of colistin as a prophylactic treatment of neutropenia in AML,<sup>21</sup> polymyxin antibiotics have the potential to simultaneously act as antibacterial and anticancer agents. However, dose-limiting neuro- and nephrotoxicity prevent their routine use,<sup>22</sup> which may be overcome by polymer conjugation, as we have shown in our previous work, where dextrin-colistin conjugates reduced toxicity in vitro and in vivo, and extended plasma half-life.<sup>11,23,24</sup> Our recent studies have demonstrated that conjugation of dextrin to colistin reduced cellular internalization of the antibiotic by kidney cells and caused reduced cytotoxicity.<sup>25</sup> In parallel, dextrin conjugation to colistin dramatically diminished both proximal tubular injury and renal accumulation of colistin in mice receiving twice-daily doses of the antibiotic. Therefore, we hypothesized that dextrin-colistin conjugates may be repurposed as an anticancer therapy, offering improved biodistribution, sustained drug exposure and reduced side-effects.

Polymer conjugation has been widely used as a means of improving drug delivery.<sup>26,27</sup> However, while polymer-protein and -peptide conjugation has shown particular success for their delivery to extracellular targets, intracellular delivery has proven to be more challenging.<sup>28</sup> Our previous studies have shown that dextrin conjugation has a varying

effect on intracellular uptake of a drug, while attachment of dextrin to PLA2 significantly increased the proportion of internalized PLA2 by MCF-7 breast cancer cells,<sup>29</sup> less colistin internalization in HK-2 proximal tubule cells was observed when conjugated to dextrin.<sup>25</sup> Therefore, it was important to establish whether conjugation of colistin to dextrin would alter its endocytic properties in AML cells.

The aim of this study was to investigate and quantify the intracellular delivery of 4 different dextrin–colistin conjugates (containing 8000 or 51,000 g/mol dextrans, having 1 or 10 mol% succinylation) to demonstrate whether dextrin conjugation can enhance colistin's anticancer activity. To achieve this, *in vitro* cytotoxicity, cellular uptake, and localization of fluorescently labelled conjugates were assessed in three leukemia cell lines.

## Materials and Methods

### Materials

Type I dextrin from corn ( $M_w = 8000$  g/mol, degree of polymerization (DP) = 50), colistin sulfate, N-hydroxysulfosuccinimide (sulfo-NHS), dimethyl sulfoxide (DMSO), dimethylformamide (DMF), Hoechst 33342 solution and staurosporine were purchased from Sigma-Aldrich (Poole, UK). Dextrin ( $M_w 51,000$  g/mol, DP = 315) was from ML Laboratories (Liverpool, UK). Disodium hydrogen phosphate, potassium dihydrogen phosphate, potassium chloride, 4-dimethylaminopyridine (DMAP), BCA protein assay kit, N,N'-dicyclohexyl carbodiimide (DCC), 1-ethyl-3-(3-(dimethylamino)propyl carbodiimide hydrochloride) (EDC), AlexaFluor<sup>®</sup> 594 (AF594) cadaverine, AF594 succinimidyl ester, sodium chloride, Gibco<sup>™</sup>-branded keratinocyte serum-free medium (K-SFM) with L-glutamine, epidermal growth factor (EGF), bovine pituitary extract (BPE), 0.05% w/v trypsin-0.53 mM EDTA, Iscove's modified Dulbecco's medium (IMDM) with GlutaMAX<sup>™</sup>, fetal bovine serum (FBS) and Roswell Park Memorial Institute (RPMI) 1640 medium with GlutaMAX<sup>™</sup> were obtained from ThermoFisher Scientific (Loughborough, UK). CellTiter-Blue<sup>®</sup> (CTB) cell viability assay kit, CytoTox-One<sup>™</sup> homogeneous membrane integrity assay kit and Caspase-Glo<sup>®</sup> 3/7 assay system kit were from Promega, WI, USA. Recombinant human granulocyte-monocyte colony stimulating factor (rhGM-CSF) was from Peprotech (London, UK). Pullulan gel filtration standards ( $M_w = 180\text{--}788,000$  g/mol) were purchased from Polymer Laboratories (Church Stretton, UK) and Shodex (Tokyo, JP). Unless otherwise stated, all chemicals were of analytical grade and used as received. All solvents were of general reagent grade (unless stated) and were from Fisher Scientific (Loughborough, UK).

### Synthesis and Characterization of Dextrin–Colistin Conjugates and AF594-Labelled Probes

Amide-linked dextrin–colistin conjugates, containing dextrin ( $M_w = 8000$  or 51,000 g/mol) with 1 and 10 mol% succinylation, were synthesized using EDC and sulfo-NHS and characterized as described previously.<sup>11</sup> To synthesize ester (E)-linked conjugates, succinoylated dextrans (1, 2.5 and 10 mol% succinylation) were conjugated to colistin using DCC and DMAP. Briefly, for 1 mol% succinoylated dextrin, succinoylated dextrin (1000 mg, 0.125 mmol), DCC (25.5 mg, 0.25 mmol) and DMAP (7.5 mg, 0.125 mmol) were dissolved under stirring in anhydrous DMSO (10 mL) in a 50 mL round-bottomed flask, and left stirring at 21°C for 15 min. Subsequently, colistin sulphate (176 mg, 0.25 mmol) was added, and the mixture was left stirring overnight at 21°C. To stop the reaction, the mixture was poured into excess chloroform (~100 mL). Resulting precipitates were isolated by filtration and dissolved in ultrapure water ( $H_2O$ ; Milli-Q<sup>®</sup> filtered to  $18.2\text{ M}\Omega\text{ cm}^{-1}$ ) (10 mL), then stored at  $-20^\circ\text{C}$  before purification by fast protein liquid chromatography (FPLC) (AKTA Purifier; GE Healthcare, UK) using a pre-packed HiLoad Superdex 30 26/600 column equipped with a UV detector, using Unicorn 5.31 software (GE Healthcare, Amersham, UK) for data analysis.

To enable visualization of conjugates by flow cytometry and confocal microscopy, succinoylated dextrin, colistin and dextrin–colistin conjugate were fluorescently labelled with AlexaFluor<sup>®</sup> 594 (AF594) and characterized according to previously published methods,<sup>29–31</sup> including spectrophotometric and fluorometric analysis. Briefly, to prepare AF594-labelled colistin, the antibiotic (16.5 mg) was solubilized under stirring in PBS (1 mL, pH 7.4) in a 10 mL round-bottomed flask. AF594 succinimidyl ester (9.5 mg, from a stock solution of 10 mg/mL in anhydrous DMF, stored at  $-20^\circ\text{C}$  until use) was added dropwise. The reaction mixture was then stirred at room temperature and protected from light. After 1 h, the solution was purified by FPLC (as above) using a prepacked Superdex 30 26/600 column coupled



with a UV detector set at 210, 280 and 550 nm. The reaction mixture (5 mL) was injected into a 5 mL loop and eluted using 0.1 M ammonium acetate (pH 6.9, 0.22  $\mu\text{m}$  filter-sterilized) at a flow rate of 2.5 mL/min. Fractions (15 mL) containing colistin-AF594 (typically between 230 and 290 mL) were identified by HPLC-fluorescence, then pooled and desalted by freeze-drying ( $\times 5$ ) to remove ammonium acetate. The final compound was stored at  $-20^{\circ}\text{C}$  until use. To prepare AF594-labelled dextrin, succinoylated dextrin (160 mg, 8000 g/mol, 10 mol%) was dissolved under stirring in a PBS buffer (5 mL, pH 7.4) in a 10 mL round-bottomed flask. To this, EDC (18.9 mg) and sulfo-NHS (21.4 mg) were added, and the mixture stirred for 15 min before addition of AF594 cadaverine (8 mg, from a stock solution of 10 mg/mL in anhydrous DMF, stored at  $-20^{\circ}\text{C}$  until use). The reaction mixture was stirred in the dark for 5 h prior to purification by size-exclusion chromatography (SEC, disposable PD-10 desalting column containing Sephadex G-25). To prepare the AF594-labelled dextrin–colistin conjugate with 10 mol% succinoylation, a dextrin-AF594 intermediate was prepared, as described above, conjugated to colistin and purified by FPLC, as previously described.<sup>11</sup> As 1 mol% succinoylated 8000 g/mol dextrin would not contain sufficient reactive groups to attach both, colistin and AF594, to prepare AF594-labelled dextrin–colistin conjugate with 1 mol% succinoylation, a colistin-AF594 intermediate was initially prepared, as above, and subsequently conjugated to 1 mol% succinoylated dextrin and purified as previously described.<sup>11</sup>

The total AF594 content of AF594-labelled dextrin and dextrin–colistin conjugates was determined by measuring absorbance at 485 nm. Free AF594 content was assessed by measuring fluorescence ( $\lambda_{\text{ex}} = 588 \text{ nm}$ ,  $\lambda_{\text{em}} = 612 \text{ nm}$ , gain 1000) of fractions (1 mL) eluting from a PD-10 column, according to previously described methods.<sup>31</sup> Analysis of colistin-AF594 was performed using LC-MS on a Synapt G2-Si quadrupole time-of-flight (QTOF) mass spectrometer (Waters, U.K.), operating in the positive electrospray ionization mode, coupled to an ACQUITY H-Class UPLC system (Waters, Wilmslow, UK). Separation was accomplished using an ACQUITY UPLC BEH column (1.7  $\mu\text{m}$ ,  $2.1 \times 100 \text{ mm}$ , Waters) inside a column oven at  $40^{\circ}\text{C}$ . A multistep gradient method was used (0–2 min, 98% A; 2–20 min, 2% A; flow rate 0.3 mL/min), where mobile phase A is water (0.1% formic acid), and mobile phase B is acetonitrile (0.1% formic acid). Analysis of the purity of AF594-labelled dextrin and dextrin–colistin conjugates was performed using PD-10 columns (Cytiva, Little Chalfont, UK), by analysis of SEC fractions for fluorescence and protein content (by BCA reagent).

## Hemolytic Activity

All animal experiments were conducted according to the United Kingdom Use of Animals (Scientific Procedures) Act 1986. Animal work was reviewed by the Animal Welfare and Ethical Review Body under the Establishment License held by Cardiff University and authorized by the UK Home Office. Fresh blood was extracted from recently euthanized male Wistar rats ( $\sim 250 \text{ g}$  body weight) by cardiac puncture and added to 4 mL PBS (pH 7.4) in a heparin/lithium blood tube. The tube was centrifuged at  $400 \times g$  for 10 min at  $4^{\circ}\text{C}$  to extract red blood cells (RBCs), then washed a further two times. Following the final wash, the RBC pellet was diluted to 2% w/v with PBS. Subsequently, this diluted RBC suspension was added to a 96-well plate (100  $\mu\text{L}$ /well, replicates  $n=6$ ) containing an equal volume of test compounds, PBS (negative control) or Triton X-100 (1% v/v) (positive control). Following incubation for 1 h at  $37^{\circ}\text{C}$ , the plate was centrifuged at  $400 \times g$  for 10 min at  $4^{\circ}\text{C}$ . The supernatant (100  $\mu\text{L}$ ) of each well was transferred to a 96-well plate, and absorbance at 550 nm was read using a Fluostar Omega microtiter plate reader. Cells were plated with 6 technical replicates per plate ( $n=6$ ) and each experiment was performed three times. The negative control (PBS) absorbance was subtracted, and the results were expressed as mean percentage of maximum (Triton X-100) hemoglobin released  $\pm 1\text{SD}$  ( $n=6$ ).

## Cell Culture

Human kidney proximal tubule cells (HK-2) and the leukemia cell lines MV-4-11 and TF-1 were obtained from ATCC (Manassas, USA). The leukemia cell line THP-1 was from ECACC (UK Health Security Agency). Characteristics of the cell lines used are shown in [Table S1](#). Cells were screened to be free of mycoplasma contamination upon thawing and monthly thereafter using a Venor GeM Classic Mycoplasma Detection Kit from Minerva Biolabs (Berlin, Germany). Cell lines were maintained in log-phase proliferation at  $37^{\circ}\text{C}$  with 5%  $\text{CO}_2$ /air and cultured in their respective culture medium ([Table S1](#)). HK-2 cells were passaged using 0.05% w/v trypsin-0.53 mM EDTA.<sup>32</sup>

## Evaluation of in vitro Cytotoxicity

Cytotoxicity of colistin sulfate and the dextrin–colistin conjugates was assessed in the above cell lines using a multiplexed assay system, to measure cell viability, membrane integrity (lactate dehydrogenase (LDH) release), caspase activity/apoptosis and DNA content as described previously.<sup>33</sup> In summary, cells were seeded into sterile black, clear-based 96-well microplates (HK-2 at 2500 cells/well; all other cell lines at 10,000 cells/well in 0.1 mL of complete media). Cultures were incubated at 37°C with 5% CO<sub>2</sub> for 1 h (MV-4-11, THP-1, TF-1) or, to allow adherent cells to adhere, for 24 h (HK-2). Test compound stock solutions were prepared in PBS (0.22 µm filter-sterilized) and used to supplement the complete media. Test compounds were evaluated in triplicate at concentrations up to 1 mg/mL colistin base with respective vehicle-only control (PBS), while 1–10 µM staurosporine (apoptosis) and 100 µM Triton-X100 (necrosis) were used as positive controls.

Following a further 24 or 72 h incubation, plates were processed as follows, protected from light throughout. To measure necrosis, 25 µL of supernatant from each well was transferred to a fresh black 96-well microplate, containing 25 µL of CytoTox-One™ assay reagent. The cultures were gently mixed, incubated at 21°C for 10 min, then a “stop solution” was added and fluorescence measured at  $\lambda_{\text{ex}} = 560 \text{ nm}$ ,  $\lambda_{\text{em}} = 590 \text{ nm}$  using a Fluostar Omega microplate reader. Total cellular LDH activity was measured after the addition of LDH lysis solution to cells, prior to addition of the assay reagent. Next, to measure cytotoxicity and DNA content, CTB reagent was supplemented with Hoechst 33,342 (100 µg/mL) and added to the wells of the original microplate (10 µL/well). Cultures were gently mixed, followed by incubation at 37°C with 5% CO<sub>2</sub> in air for 1 h and fluorescence measured at  $\lambda_{\text{ex}} = 560 \text{ nm}$ ,  $\lambda_{\text{em}} = 590 \text{ nm}$  and  $\lambda_{\text{ex}} = 340 \text{ nm}$ ,  $\lambda_{\text{em}} = 460 \text{ nm}$  (for cytotoxicity and DNA content, respectively) using a Fluostar Omega microplate reader. Finally, 60 µL of Caspase-Glo 3/7 assay reagent was added to each well of the original microplate. Plates were gently agitated and then incubated at 20°C with 5% CO<sub>2</sub> in air for 1 h, followed by luminescence assays using a Fluostar Omega microplate reader. The cells were plated with 3 technical replicates per plate (n=3) and each experiment was performed twice. Data was corrected for no-cell background, then expressed as mean percentage of the response of vehicle-only control cells  $\pm 1\text{SD}$  (n=3). Relative IC<sub>50</sub> values were determined using a non-linear regression analysis of dose-response-inhibition using a 4-parameter logic model in GraphPad Prism (version 9.3.1, 2021; San Diego, CA, USA).

To monitor apoptosis and necrosis continuously over 72 h, a RealTime-Glo™ Annexin V apoptosis and necrosis assay (Promega, Southampton, UK) was used. Briefly, MV-4-11 cells were plated into sterile black, clear-based 96-well microplates (4500 cells/well in 45 µL of complete media). Test compound solutions (10 µL) and 2x detection reagent (55 µL) were added to each well, in triplicate, and the plate was gently agitated before placing inside a Fluostar Omega plate reader (maintained at 37°C with 5% CO<sub>2</sub>). Fluorescence ( $\lambda_{\text{ex}} = 485 \text{ nm}$ ,  $\lambda_{\text{em}} = 525\text{--}530 \text{ nm}$ ) and luminescence were measured at regular time points for up to 72 h. Data was corrected for no-cell background and expressed as a percentage of the response of vehicle-only control cells. Staurosporine and Triton-X100 were used as positive controls for apoptosis and necrosis, respectively, as described above. The cells were plated with 3 technical replicates per plate (n=3) and each experiment was performed once.

## Cell Cycle Analysis

Cell cycle analysis of MV-4-11 cells following incubation with colistin sulfate, DC8/1 or DC8/10 at the previously determined IC<sub>50</sub> value was performed according to a modified version of Ormerod's protocol.<sup>34</sup> Briefly, 500 µL cells at 10<sup>5</sup> cell/mL per well of a 24-well plate were incubated in complete media supplemented with test compounds (in duplicate) at their IC<sub>50</sub> value at 37°C with 5% CO<sub>2</sub> for 24 h. The contents of each well were diluted with 3 mL PBS, then centrifuged (350 × g for 5 min at 20°C), the cell pellet was resuspended in ice-cold PBS then centrifuged again prior to removing the supernatant. Subsequently, ice-cold 70% v/v ethanol was added dropwise under vortex to resuspend the cells, which were then incubated on ice. Following 30 min, cells were centrifuged (450 × g for 10 min at 4°C) then washed twice with ice-cold PBS, vigorously resuspending the pellet each time. To the cell pellet, 50 µL of RNase (100 µg/mL) solution was added then incubated at 37°C for 15 min. Finally, 200 µL of propidium iodide (PI; 50 µg/mL) solution was added to each tube 20 min prior to data acquisition with a Becton Dickinson FACS CANTO II Cell Analyser flow cytometer equipped with a 488 nm blue laser and a 584/42 nm emission filter. Data were collected for

25,000 events per sample and data analyzed using FlowJo™ software, v10.8.1. MV-4-11 cells incubated with medium only were used to determine background fluorescence. Cell fragments, clumps and debris were excluded using sequential gating on a forward-scatter (FSC)-height vs side-scatter (SSC)-height cytogram and a DNA (FL2)-area vs DNA (FL2)-width cytogram, then the remaining single cells were displayed in a histogram of DNA-area (FL2), as described by Ormerod; the Watson (pragmatic) algorithm, a univariate cell cycle model, was employed to assess the proportion of cells in each cell cycle phase: G1, S and G2(M)<sup>35</sup> using FlowJo™ software (version 10.8.1). The cells were plated with 2 technical replicates per plate (n=2) and each experiment was performed four times.

## Colony Formation

Colony-forming ability of MV-4-11 and THP-1 cells following incubation with colistin sulfate, DC8/1 or DC8/10 at the previously determined IC<sub>50</sub> value was measured using a human Colony Forming Cell (CFC) assay in methylcellulose-based media, according to manufacturer's instructions (R&D Systems, Abingdon, UK). Briefly, cells (10<sup>5</sup> cells/mL) were incubated in complete media supplemented with 10% v/v test compounds at their IC<sub>50</sub> value or with vehicle (PBS) at 37°C with 5% CO<sub>2</sub> for 24 h. Then, the equivalent of 667 THP-1 or 400 MV-4-11 cells were added in duplicate to 1 mL human methylcellulose base media supplemented with recombinant human granulocyte-monocyte colony stimulating factor (10 ng/mL), interleukin-3 (10 ng/mL) and stem cell factor (20 ng/mL) in a 35 mm culture dish (Nunclon, Fisher Scientific). Following the incubation at 37°C with 5% CO<sub>2</sub> for 10 days, colonies containing >32 cells were enumerated by inverted light microscopy. The results were expressed as mean percentage colony-forming units (CFU) of vehicle-only control (n=2).

## Determination of Cellular Uptake

To investigate cell association at 4 or 37°C, leukemia cells were first resuspended at 200,000 cells/well of a 96-well plate in 75 µL complete medium (without phenol red). Experiments at 37°C were conducted with standard cell culture conditions, but for low-temperature experiments, cells were pre-incubated for 30 min at 4°C prior to the addition of the probe. Solutions of fluorescent probes were freshly prepared in a complete medium at sub-toxic, equivalent concentrations of AF594 base (1 µg AF594 base/mL), filter-sterilized (0.22 µm), then equilibrated to either 37 or 4°C for 30 min. Probe solutions were added to each well (75 µL) containing cells and incubated at 4 or 37°C for 2 h. Subsequently, plates were placed on ice before transferring the cell suspension into individual tubes and washing twice by centrifugation (350 × g, 5 min) with ice-cold PBS (2 × 3 mL). Finally, the cells were resuspended in ice-cold PBS (200 µL) prior to data acquisition using a Becton Dickinson LSR Fortessa Cell Analyser flow cytometer equipped with a yellow-green laser (561 nm) and emission filter for 585/15 nm. For each sample, 10,000 events were collected and analyzed using FlowJo™ software v 10.8.1. Control cells incubated with medium only were used to determine background fluorescence. Throughout, the results were corrected for cell autofluorescence and expressed as (geometric mean × % positive cells)/100, where % positive cells was calculated as 100 – % cells in M1. Internalization was calculated by subtracting the cell-associated fluorescence at 4°C (extracellular binding) from that at 37°C (intracellular uptake plus extracellular binding) and expressed as mean ± SD. All uptake studies were performed using colistin concentrations that have previously been shown to be non-toxic. The cells were plated with three technical replicates per plate (n=3); each experiment was performed three times. The results are expressed as mean fluorescence ± 1SD (n=3).

## Intracellular Localization

Cells were incubated in complete media (without phenol red, at 6.67 × 10<sup>5</sup> cells/mL) containing dextran-AF488 (150 µg/mL) at 37°C with 5% CO<sub>2</sub> /in air. After 3 h, excess dextran-AF488 was removed by addition of complete media (10x labelling volume) followed by centrifugation at 350 × g for 5 min. The cell pellet was then resuspended in complete media (10<sup>5</sup> cells/150 µL) with and without AF594 probes (5 µg AF594 base/mL) and incubated at 37°C with 5% CO<sub>2</sub> for 2 h in 96-well plates. In all cases, colistin concentration was below IC<sub>50</sub>. The cells were washed twice with 10x volume complete medium, as described above. After the final wash, 10<sup>5</sup> cells/mL cells were cultured in fresh medium at 37°C with 5% CO<sub>2</sub> for a further 2 h (short chase) or overnight (16 h, long chase). Control cells (not incubated with a probe) were used to account for autofluorescence.

Confocal laser scanning microscopy was performed using a Leica SP5 system (37°C, 5% CO<sub>2</sub>). Confocal imaging was performed sequentially with the 405 nm (Hoechst 33,342) and 543 nm (AF594) lasers captured concurrently and 488 nm (AF488) laser captured sequentially between lines. Images were captured using a HCX PL APO CS 100.0 × 1.40 oil immersion objective at 400 Hz with a line average of 3 (bi-directional scanning), with the pinhole set to 1 airy unit. Images were acquired with a raster size of 1024 × 1024 and a zoom of 1.12 to give an apparent pixel size of 138 × 138 nm (XY). At least eight representative images (single section) were obtained from each sample; typical results are shown. Images were analyzed and processed using ImageJ.<sup>36</sup>

## Statistical Analysis

GraphPad Prism (version 9.3.1, 2021; San Diego, CA, USA) software was used to perform statistical analyses. Statistical significance is indicated by \*  $p < 0.05$ , \*\*  $p < 0.01$ , \*\*\*  $p < 0.001$  and \*\*\*\*  $p < 0.0001$ . One-way analysis of variance (ANOVA) was used to evaluate multiple group comparisons ( $n \geq 3$ ) followed by Dunnett's post hoc test to account for multiple comparisons, unless otherwise stated.

## Results

Amide- and ester-linked dextrin–colistin conjugates (containing 8000 or 51,000 g/mol dextrans, having 1 or 10 mol% succinylation) were synthesized to compare their in vitro cytotoxicity and colony-forming ability of treated cells. Fluorescent dextrin, colistin and dextrin–colistin conjugate were subsequently obtained by chemical attachment of AF594 to enable measurement of cellular uptake and localization in leukemia cell lines.

## Synthesis and Characterization of Dextrin–Colistin Conjugates

The characteristics of dextrin–colistin conjugates used in these studies are summarized in Table 1. Typical FPLC chromatograms of conjugate reaction mixtures are shown in Figure S1, and overlaid with the protein content of fractions in Figure S2, to confirm successful conjugation. Free colistin content of the purified conjugates, analyzed by FPLC, was determined to be <3%.

## Hemolytic Activity

The hemolytic activity of colistin and dextrin–colistin conjugates was measured with fresh rat RBCs to assess the effect of free and dextrin-conjugated colistin on normal blood cells. After exposure of RBCs to treatments for 24 h, only the highest dose of free colistin sulfate induced significant lysis, compared to vehicle alone (Figure 1). No hemolysis was

**Table 1** Summary of the Properties of the Dextrin–Colistin Conjugates Used in This Study

Compound	Dextrin/ Succinylation	Abbreviation	Mw <sup>a</sup> (g/mol) (Mw/Mn)	Colistin Content (% w/w)	Molar Ratio of Dextrin (Per Colistin)
Dextrin-amide-colistin conjugate	8000 g/mol, 1 mol%	DC8/1	11,500 (2.3) 13,800 (2.3)	4.89 6.03	3.65 2.93
	8000 g/mol, 10 mol%	DC8/10	35,000 (3.2) 39,500 (3.7)	14.21 16.41	1.13 0.96
	51,000 g/mol, 1 mol%	DC51/1	49,000 (1.8) 48,200 (2.9)	6.08 2.21	0.43 1.22
	51,000 g/mol, 10 mol%	DC51/10	52,500 (2.4) 59,000 (2.6)	13.07 12.41	0.18 0.19
Dextrin-ester-colistin conjugate	8000 g/mol, 1 mol%	DC8/1e	7200 (2.0)	2.50	7.32
	8000 g/mol, 10 mol%	DC8/10e	19,200 (4.9)	3.24	5.61

**Notes:** <sup>a</sup>Relative to pullulan standards, using TSK G4000PW<sub>XL</sub> and G3000PW<sub>XL</sub> columns in series.

**Abbreviations:** g/mol, gram per mole; mol, mole; Mw, weight average molecular weight; g/mol, gram per mole; Mn, number average molecular weight; Mw/Mn, polydispersity; w/w, weight in weight; DC, dextrin–colistin; e, ester.

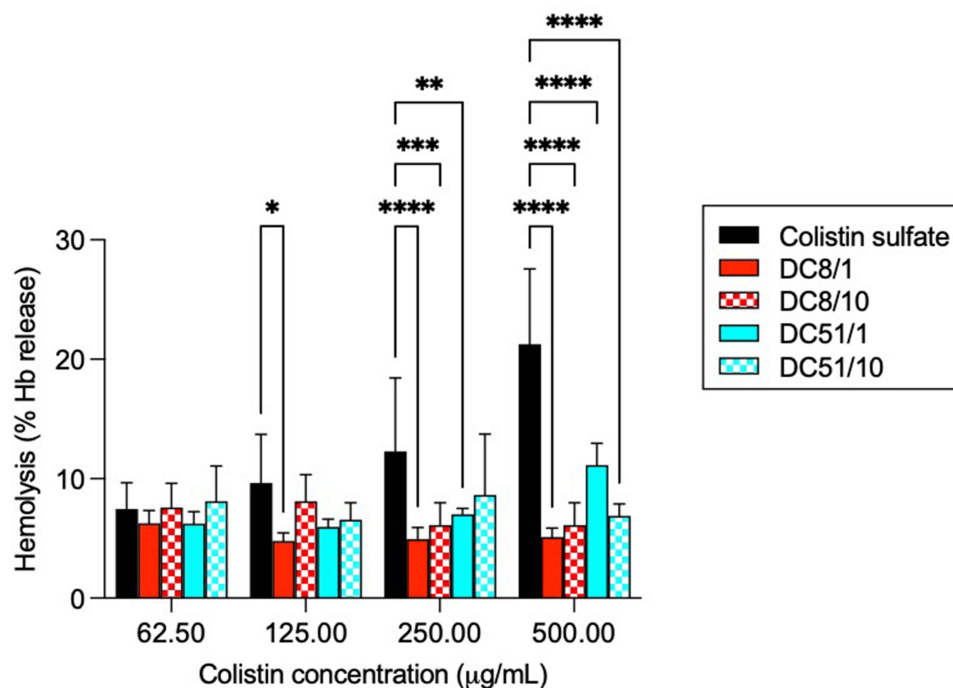


**Figure 1** Hemolysis of rat erythrocytes following incubation for 24 h with colistin sulfate and dextrin–colistin conjugates at 37°C. Data is expressed as mean % Triton X-100 control  $\pm$  1SD, n = 6. \*Indicates significance  $p < 0.05$ , \*\*Indicates significance  $p < 0.01$ , \*\*\*Indicates significance  $p < 0.001$  and \*\*\*\*Indicates significance  $p < 0.0001$  compared to colistin sulfate. Where significance is not shown,  $p > 0.05$  (ns, not significant).

observed for any of the dextrin–colistin conjugates up to 500  $\mu\text{g/mL}$ . Control experiments with dextrin and succinoylated dextrans showed  $< 10\%$  hemolysis up to 10  $\text{mg/mL}$  (data not shown).

## In vitro Cytotoxicity

Cytotoxicity was determined in three representative myeloid leukemia cell lines, in comparison to a non-cancerous human kidney proximal tubular cell line. As expected, cell viability decreased with longer incubation times in all cell lines. Where inhibition at 24 h achieved at least 50%, cell viability data was used to generate relative  $\text{IC}_{50}$  values, summarized in Table 2.

Colistin sulfate exhibited greatest cytotoxicity against HK-2 cells (Figure 2a and S3a); amide-linked dextrin conjugation reduced toxicity of colistin in HK-2 by at least 1.4-fold, compared to the free drug, and was most effective in conjugates

**Table 2** Half Maximal Inhibitory Concentration ( $\text{IC}_{50}$ ) Values and Fold-Change (CTB Assay) of Colistin Sulfate and Dextrin–Colistin Conjugates After 24 h Incubation

Compound	$\text{IC}_{50}$ ( $\mu\text{g/mL}$ Colistin Base, $\pm$ SD) <sup>a</sup>			
	THP-1	TF-1	MV-4-11	HK-2
Colistin sulfate	500 $\pm$ 89	670 $\pm$ 17	888 $\pm$ 37	447 $\pm$ 67
DC8/1	396 $\pm$ 13 (0.8)	315 $\pm$ 57 (0.5)	239 $\pm$ 19 (0.3)	653 $\pm$ 78 (1.5)
DC8/10	>1000	>1000	>1000	>1000
DC51/1	724 $\pm$ 161 (1.5)	819 $\pm$ 2 (1.2)	880 $\pm$ 64 (1.0)	638 $\pm$ 19 (1.4)
DC51/10	>1000	>1000	>1000	>1000

**Notes:** <sup>a</sup>Values in parentheses correspond to fold-change, compared to colistin sulfate.

**Abbreviations:**  $\text{IC}_{50}$ , half-maximal inhibitory concentration;  $\mu\text{g/mL}$ , microgram per milligram; SD, standard deviation; DC, dextrin–colistin.



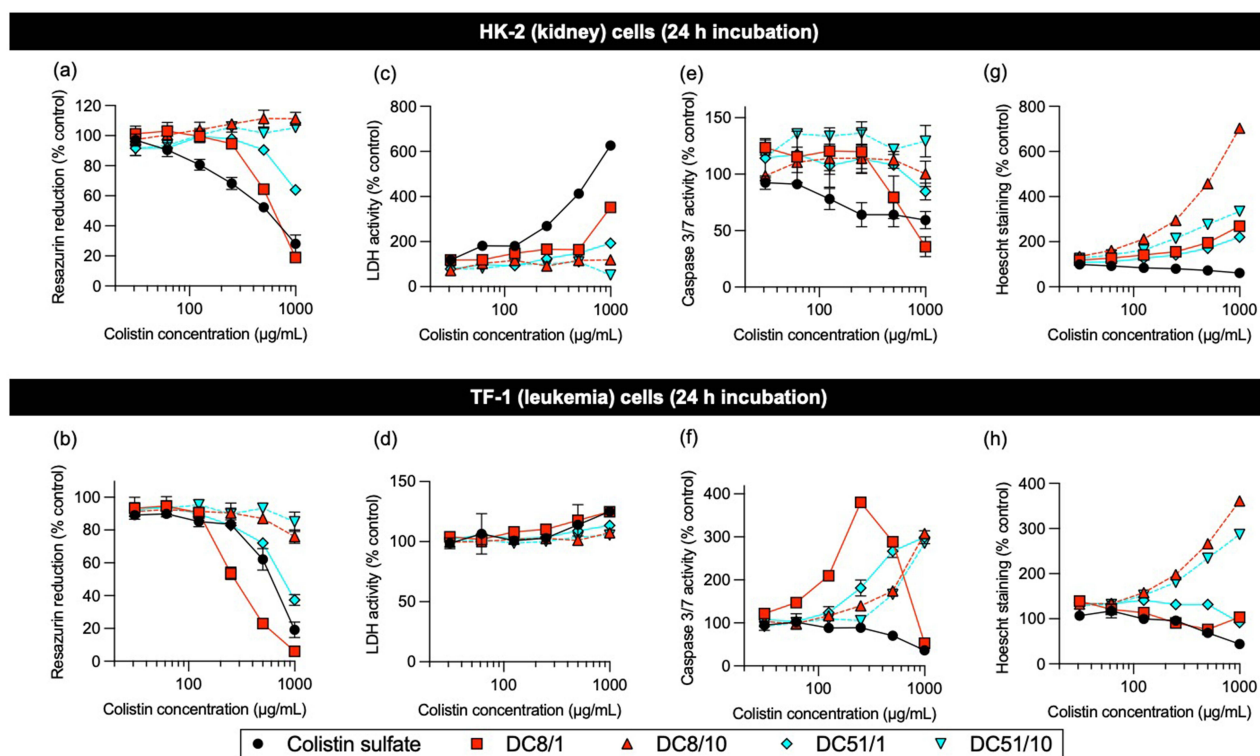


**Figure 2** Detection of resazurin reduction (metabolic activity), LDH leakage (cell-membrane integrity, necrosis), caspase 3/7 activity (apoptosis) and Hoechst 33342 staining (DNA content) under multiplex conditions of (a,c,e and g) HK-2 and (b,d,f and h) TF-1 cells incubated for 24 h with colistin sulfate and dextrin–colistin conjugates. Data represent mean ( $\pm$  ISD,  $n=3$ ). Where error bars are invisible, they are within size of data points.

containing longer dextrin chains and higher degrees of succinylation. Similarly, in the leukemia cell lines, conjugation to dextrin reduced cytotoxicity for three of the four amide-linked conjugates tested: DC8/10, DC51/1 and DC51/10 (Table 2, Figures 2b and S3b) by varying degrees. However, in all leukemia cell lines tested, DC8/1 was between 1.3–3.7-fold more potent than the free antibiotic (Table 2).

Colistin sulfate induced dose-dependent necrosis in all cell lines at 24 and 72 h (Figures 2c, d and S3c, d), with no evidence of caspase 3/7-dependent apoptosis (Figures 2e, f and S3e, f). In contrast, amide-linked conjugates showed dose-dependent caspase 3/7 activity (DC8/1 > DC51/1 > DC8/10 > DC51/10), in all leukemia cell lines at 24 h post-treatment (3.8-fold increase in caspase 3/7 activity in TF-1 cells treated with DC8/1 at 0.25 mg/mL colistin base, Figure 2f). However, by 72 h, no caspase 3/7 activity was seen. No comparable caspase 3/7 upregulation was seen in HK-2 cells for any of the treatments tested (Figures 2e and S3e). Overall, patterns of concentration-dependent cytotoxicity were similar in all leukemia cell lines tested, in contrast to non-cancerous HK-2 cells (Figure 2 and Figure S3).

Differences in concentration-dependent cell viability and apoptosis were observed between amide- and ester-linked dextrin–colistin conjugates (Figure 3). Ester-linked conjugates exhibited a similar effect on cell viability as the amide-linked DC8/1, but the latter caused the greatest increase in caspase 3/7 activity (Figure 3a and b). When cell viability and apoptosis data were plotted against the dextrin content of the respective dextrin–colistin conjugate, the cytotoxic effects became more congruent (Figure S4). DC8/1 remained the most potent amide-linked conjugate; however, there was no difference in cytotoxicity between the ester- and amide-linked conjugates. Amide-linked conjugates, however, showed more caspase 3/7 activity at equivalent dextrin concentrations, than the ester-linked conjugates. Annexin V binding occurred within a few hours of treatment and a subsequent peak in necrosis was detected (Figure 3c and d). Ester-linked DC8/1e conjugate caused less apoptosis, but more necrosis, than the amide-linked equivalent (DC8/1). Ester-linked conjugates were not tested in further experiments, due to the high batch-to-batch variability in conjugation efficiency and excessive amounts of unconjugated polymer, compared to amide-linked conjugates.



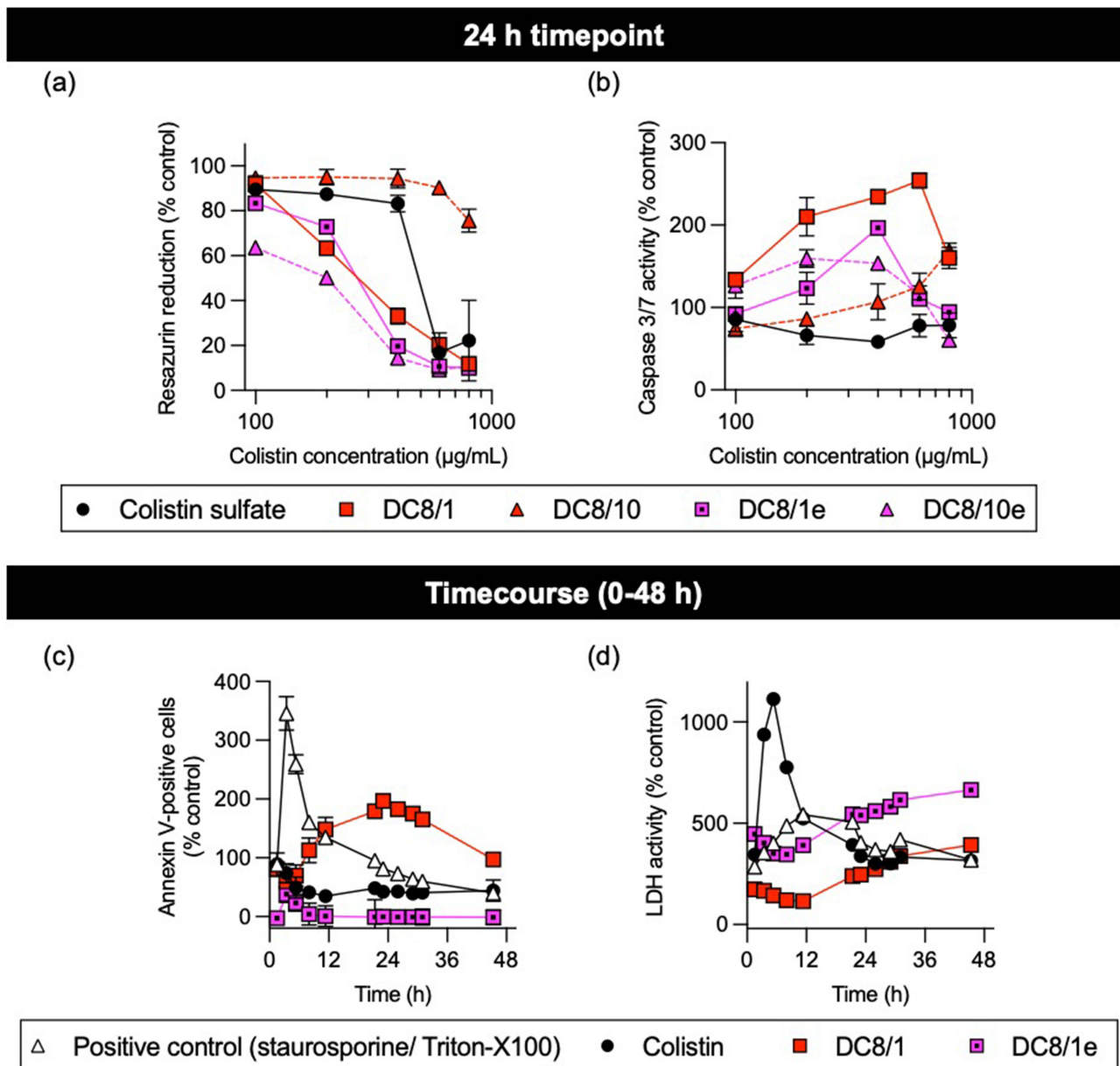


**Figure 3** Panels (a) and (b) show detection of resazurin reduction (metabolic activity) and caspase 3/7 activity (apoptosis), respectively, under multiplex conditions of MV-4-11 cells incubated for 24 h with colistin sulfate and dextrin–colistin conjugates containing amide or ester linkers. Data represent mean ( $\pm$ ISD,  $n=3$ ). Panels (c) and (d) show time course of annexin V binding and LDH activity (necrosis), respectively, during incubation of MV-4-11 cells with colistin sulfate or ester- and amide-linked dextrin–colistin conjugates at 750  $\mu$ g/mL colistin base ( $\pm$ ISD,  $n=3$ ). Where error bars are invisible, they are within size of data points.

Cells treated with DC8/10 and DC51/10 in the multiplex assay exhibited concentration-dependent increases in Hoechst 33,342 staining (Figures 2d, h and S3d, h), which suggested DNA accumulation. Subsequent cell cycle analysis using PI failed to show any significant changes in the phase distribution associated with different treatments, apart from a limited, but statistically significant, reduction in the G2M population of cells treated with DC8/1, compared to colistin sulfate (Figure 4a).

## Colony Formation

A colony formation assay was employed to determine the potential inhibitory effects of dextrin–colistin conjugates on tumor cell phenotype. Following exposure of leukemia cells to colistin sulfate at  $IC_{50}$  for 24 h, colony formation was reduced, compared to control, in both cell lines (MV-4-11:  $69\pm 10\%$ , THP-1:  $55\pm 1\%$ ) (Figure 4b and c). Inhibition of

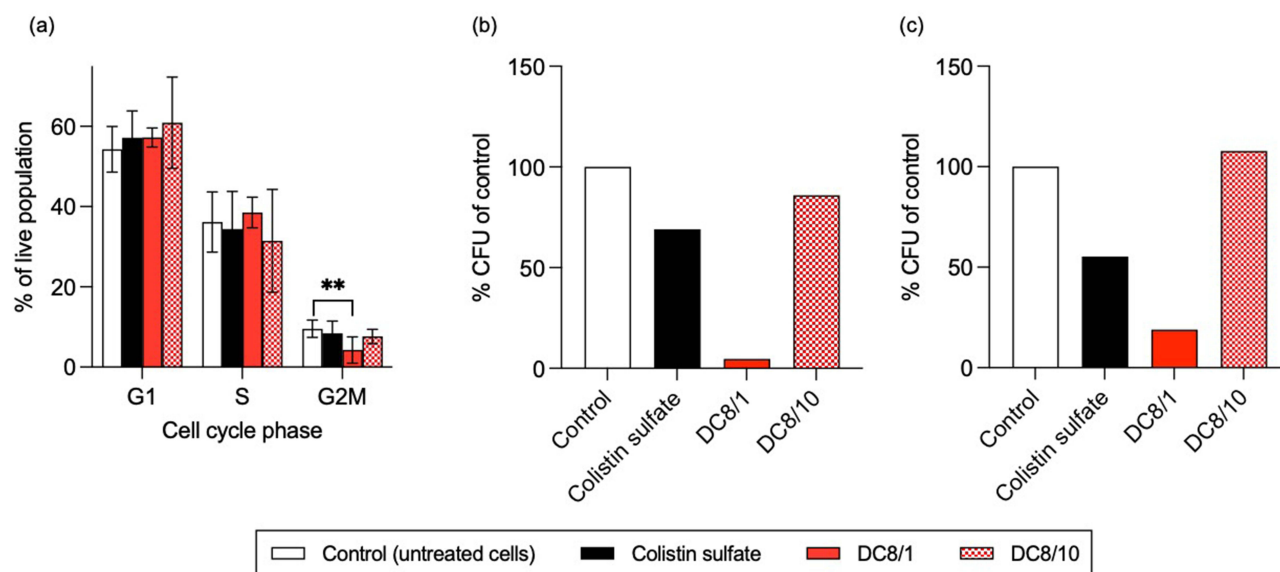


**Figure 4** Cell cycle analysis of (a) MV-4-11 cell, and colony-forming ability of (b) MV-4-11 and (c) THP-1 cells following incubation with colistin sulfate or dextrin–colistin conjugates at  $IC_{50}$  for 24 h. Data in panel (a) are presented as mean % gated population ( $\pm$ 1SD,  $n=8$ ). Data in panels (b) and (c) are presented as mean % CFU, relative to control ( $n = 2$ ). \*\*Indicates significance  $p < 0.01$ , compared to untreated control. Where significance is not shown,  $p > 0.05$  (ns, not significant). Panels (b) and (c) do not show error bars as data is  $n=2$ .

colony formation was most pronounced in cells treated with DC8/1 at the equivalent colistin dose (MV-4-11:  $4.7 \pm 1.6\%$ , THP-1:  $19 \pm 2\%$ ), while DC8/10 did not alter colony formation in either cell line tested.

## Evaluation of Cellular Uptake and Intracellular Fate

To study cellular uptake, AF594-labelled colistin, dextrin and dextrin–colistin conjugates were synthesized, containing  $<2\%$  free AF594 (Figure S5). The characteristics of all AF594-labelled probes used in these studies are summarized in Table 3.

Flow cytometry demonstrated that all AF594-labelled conjugates exhibited cell association after 1 h at  $37^\circ\text{C}$  (Figure 5 and Figure S6). In all instances, the cell-associated fluorescence was reduced at  $4^\circ\text{C}$ , indicating  $>98\%$  calculated internalization of fluorescent probes. Colistin-AF594 cellular levels were significantly greater than observed for the AF594-labelled dextrin–colistin conjugates. However, DC8/1-AF594 displayed significantly more uptake by MV-4-11 cells than DC8/10-AF594 at  $37^\circ\text{C}$  ( $p > 0.0001$ , 2-way ANOVA, Tukey's multiple comparison test).

In line with flow cytometry data, confocal microscopy showed that colistin-AF594 and AF594-labelled dextrin–colistin conjugates were internalized, with punctate labelling resembling endolysosomal structures (Figures 6 and 7). There was clear evidence that colistin-AF594 was reaching the lysosomes, manifesting as colocalization with the pulse-chased dextran. However, dextrin conjugation significantly reduced colistin internalization, exacerbated by increased succinylation.

**Table 3** Characteristics of AF594-Labelled Conjugates

Compound	Degree of Labelling (Moles AF594 per Mole Colistin/Dextrin/Dextrin–Colistin Conjugates)	Labelling Efficiency ( $\mu\text{g}$ AF594/mg Conjugate)
Colistin-AF594	0.273	135.12
Dextrin (8 kDa, 10 mol%)-AF594	0.026	2.79
DC8/1-AF594	0.036	2.29
DC8/10-AF594	0.092	2.11

**Abbreviations:** AF594, AlexaFluor 594;  $\mu\text{g}$ , microgram; mg, milligram, kDa, kilodalton; DC, dextrin–colistin.

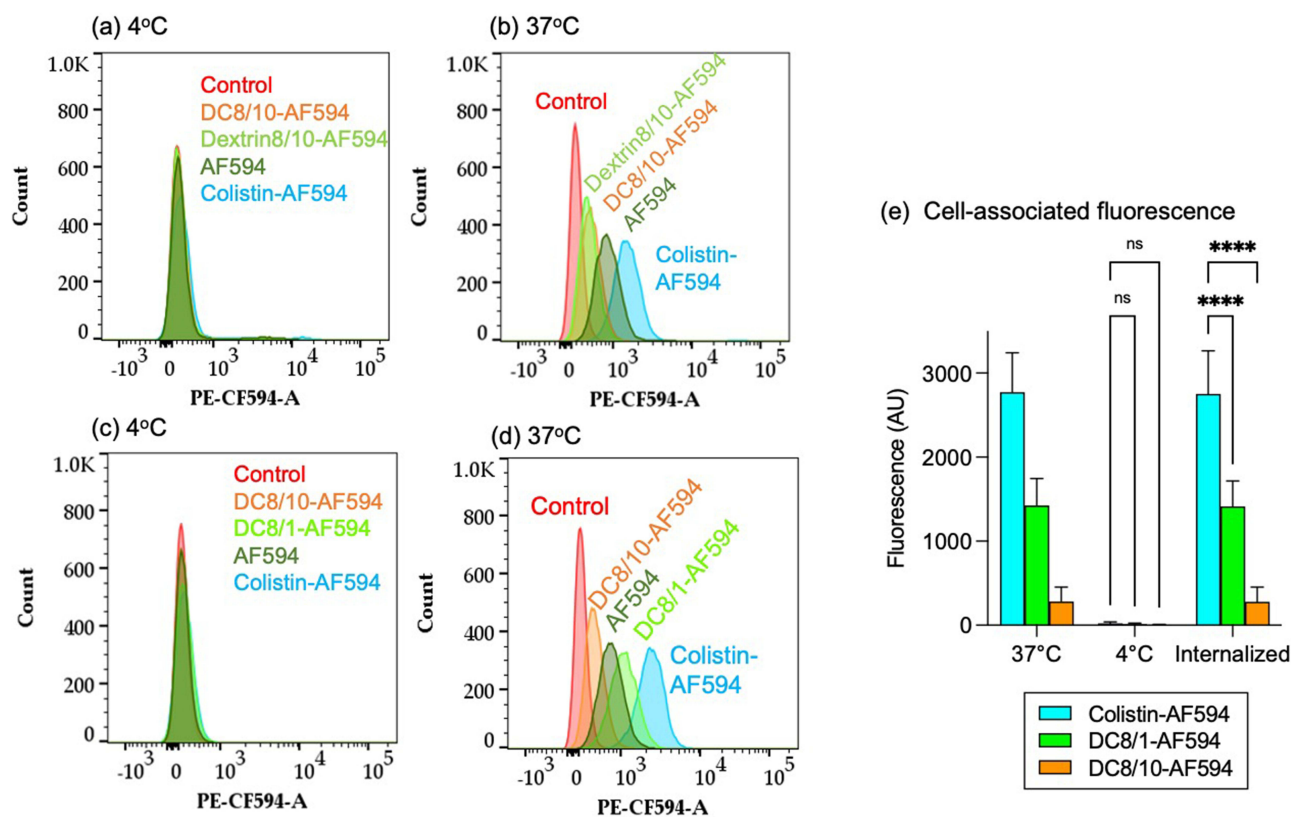


**Figure 5** Binding and internalization of AF594 (control) and AF594-labelled colistin, succinoylated dextrin (8k, 10 mol%) and dextrin–colistin conjugates by MV-4-11 cells after 1 h incubation at 4°C and 37°C. Panels (a-d) show histograms for cell-associated fluorescence at 4°C (a) and 37°C (b) and (c) and (d). Panels (a) and (b) show comparative uptake of DC8/10 compared to AF594-labelled colistin and dextrin alone. Panels (c) and (d) show a second experiment comparing the up-take of DC8/1 vs DC8/10, with appropriate controls. Panel (e) shows cell-associated fluorescence at 37°C (total association) and 4°C (external binding) of AF594-labelled colistin, dextrin and dextrin–colistin conjugates ( $\pm$  ISD,  $n = 6$ ). \*\*\*\*Indicates significance  $p < 0.0001$ , and ns (not significant) indicates  $p > 0.05$ , compared to colistin-AF594.

## Discussion

Targeted therapies, which interfere with specific proteins involved in tumorigenesis, survival and growth, are promising precision medicines for cancer.<sup>37</sup> The clinical development of targeted therapies has yielded few FDA-approved treatments for AML,<sup>38</sup> in part, due to unacceptable side effects and an inability to reach their intracellular targets. Drug delivery strategies, such as polymer therapeutics, offer the ability to overcome these issues.<sup>39</sup> LSD1/KDM1A is overexpressed in many cancers, including AML, and has a significant role in regulating differentiation, proliferation and invasion of cancer cells, making it an attractive target for AML treatment.<sup>40</sup> Speranzini et al<sup>17</sup> reported non-covalent inhibition of LSD1/KDM1A by polymyxin antibiotics, which supported a serendipitous observation by Verstovsek et al,<sup>16</sup> that polymyxin B was cytotoxic to a range of cancer cell lines, including the human acute lymphocytic leukemia cell line, REH ( $IC_{50} = \geq 20$   $\mu\text{g/mL}$ ).

Here, we showed that colistin sulfate was less cytotoxic to leukemia cell lines than a normal kidney cell line. HK-2 cells were used as non-cancerous cells for comparison due to their consistent response to dextrin–colistin conjugates in previous studies.<sup>25</sup> However, it would also be useful, in future studies, to perform these experiments in CD34+ cells from healthy donors to further substantiate our findings in leukemia and healthy kidney cells. When Speranzini et al<sup>17</sup> treated MV-4-11 cells with colistin, they did not observe any significant alteration in cell growth or H3-Lys<sup>4</sup>/H3-Lys<sup>9</sup> methylation. However, this study used a relatively low concentration of colistin sulfate (1.2  $\mu\text{g/mL}$ , 0.85  $\mu\text{M}$ ), given that our study found an  $IC_{50}$  of this agent in the same cells to be 888  $\mu\text{g/mL}$  (768.5  $\mu\text{M}$ ). In contrast, other LSD1 inhibitors have shown substantially higher activity towards AML cell lines, for example, tranlycypromine-based compounds developed by Fioravanti et al had  $IC_{50}$  values of 0.4 and 2.5  $\mu\text{M}$  in MV-4-11 cells (48 h incubation)<sup>41</sup> and the LSD1 inhibitor, IMG-7289 had an  $IC_{50}$  values of 0.007  $\mu\text{M}$  in the same cell line (48 h incubation).<sup>42</sup>



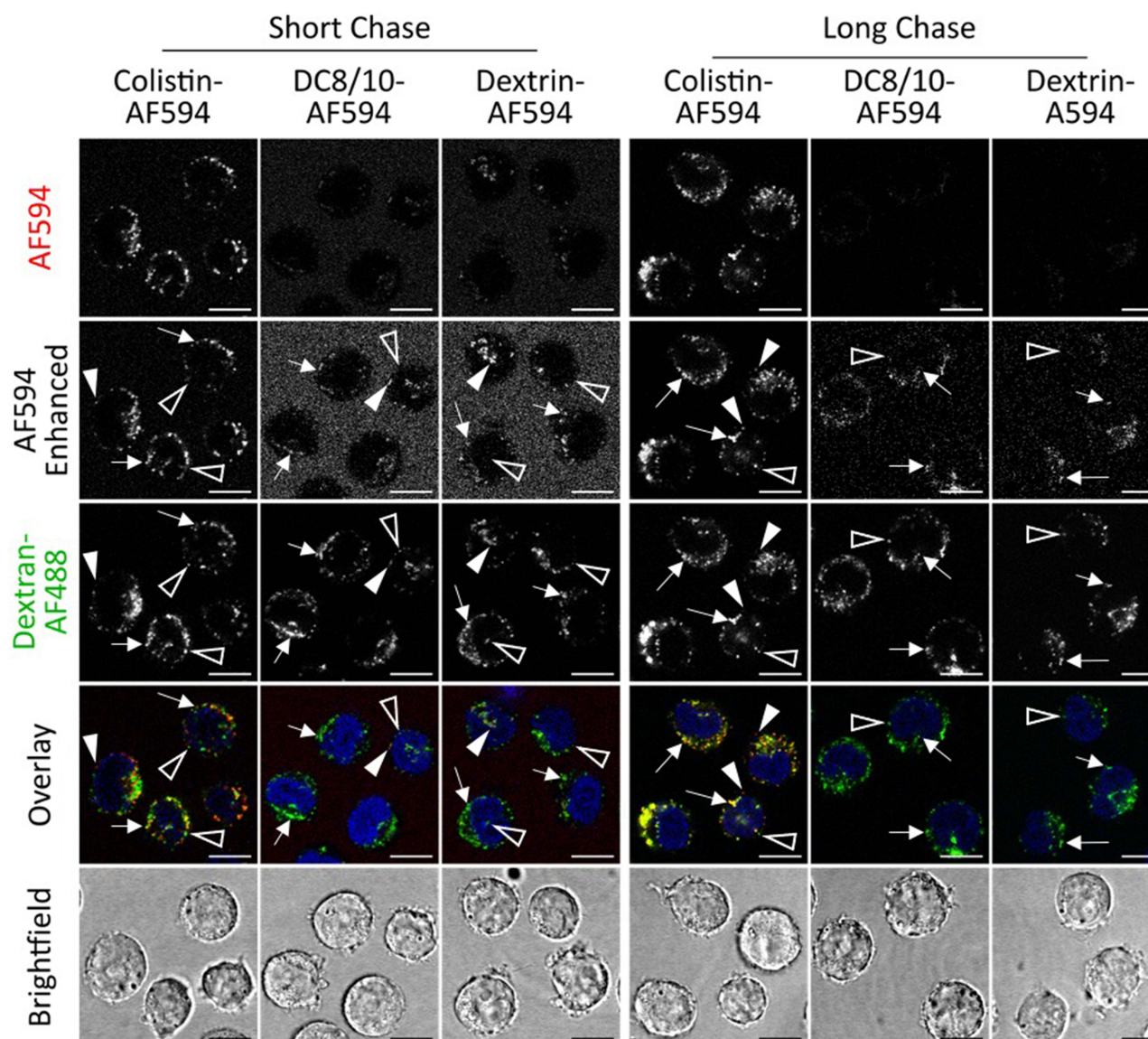


**Figure 6** Uptake of Colistin-AF594, DC8/10-AF594 and Dextrin-AF594 (8k/10%) following a 2 h pulse and either 2 h (short) or 16 h (long) chase in MV-4-11 cells. Dextran-AF488 (green) was used to identify late endolysosomes and Hoechst 33,342 (blue) was used as a nuclear marker. Scale bar shows 10  $\mu$ m. Arrows indicate colocalised cargo and lysosomal dextran, solid arrow heads indicate non-colocalised cargo and hollow arrow heads indicate non-colocalised lysosomal dextran. Image intensities have been adjusted so that differences in colocalisation can be more evenly compared. All images are single sections.

Speranzini et al hypothesized that colistin was unable to cross the plasma membrane efficiently; however, we showed here that fluorescently labelled colistin was rapidly endocytosed by all 3 leukemia cell lines tested, with compelling evidence of further traffic to lysosomes. Contrary to our initial hypothesis, however, dextrin conjugation reduced internalization of colistin by leukemia cells, but did not alter its intracellular localization or promote nuclear localization.

Although all leukemia cell lines tested had similar mRNA expression of KDM1A mRNA expression (summarized in [Table S1](#)),<sup>43</sup> the relative cytotoxicity of colistin sulfate or dextrin–colistin conjugates varied between the leukemia cell lines tested; MV-4-11 showing the largest reduction in  $IC_{50}$  for DC8/1 (4-fold lower). Cellular uptake of fluorescently labelled compounds was similar for all three leukemia cell lines tested, suggesting that inconsistent internalization across the cell lines was not the cause of sensitivity differences.

When dextrin was conjugated to colistin, variable effects on cytotoxicity were observed, which were dependent on dextrin chain length, degree of succinylation and type of linker used. The most potent effect seen in leukemia cell lines was from dextrin–colistin conjugates containing 8000 g/mol dextrin, with 1 mol% succinylation and attached to colistin

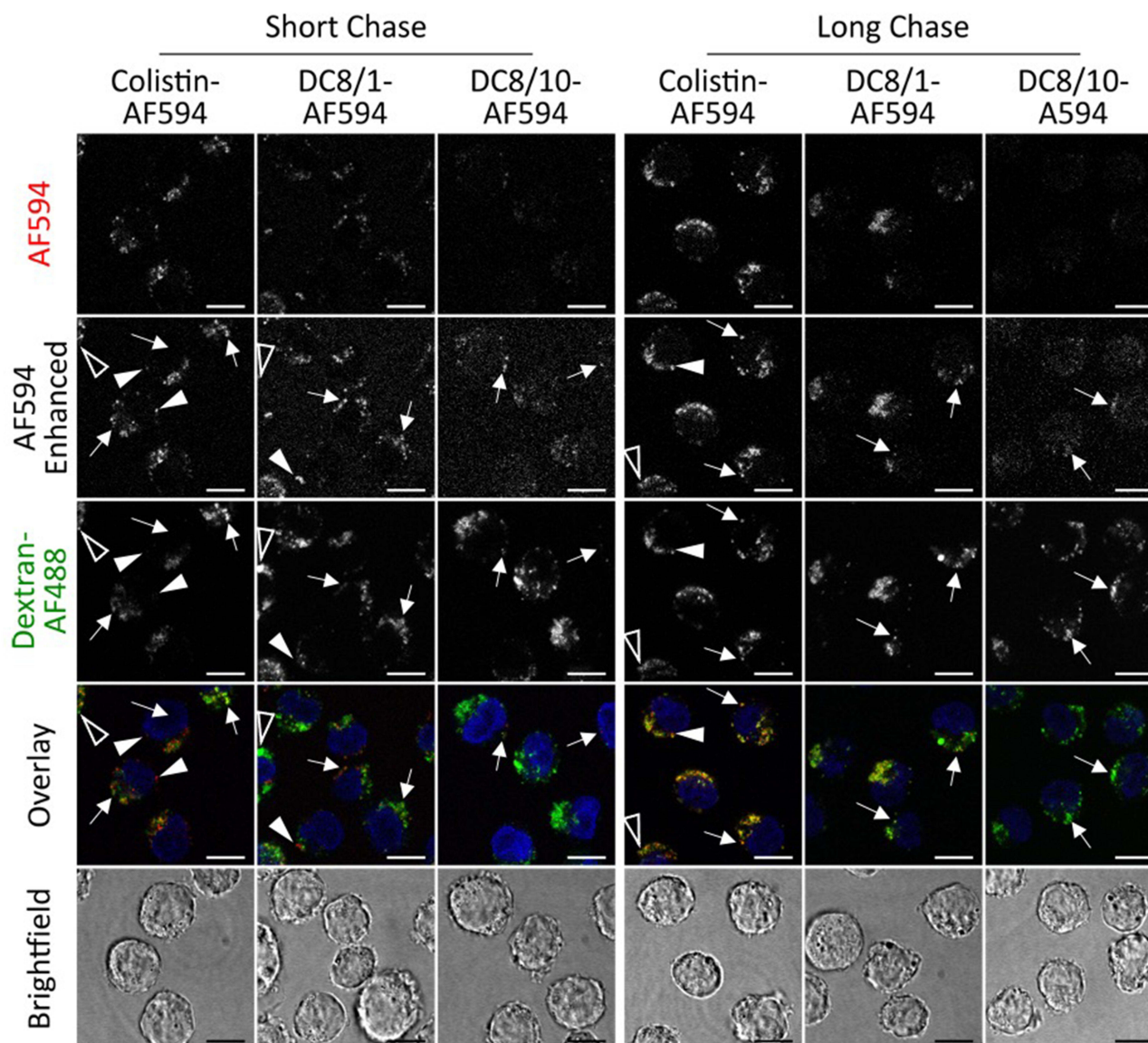


**Figure 7** Uptake of colistin-AF594, DC8/1-AF594 and DC8/10-AF594 following a 2 h pulse and either 2 h (short) or 16 h (long) chase in MV4-11 cells. Dextran-AF488 (green) was used to identify late endolysosomes and Hoechst 33,342 (blue) was used as a nuclear marker. Scale bar shows 10  $\mu$ m. Arrows indicate colocalised cargo and lysosomal dextran, solid arrows indicate non-colocalised cargo and hollow arrow heads indicate non-colocalised lysosomal dextran. Image intensities have been adjusted so that differences in colocalisation can be more evenly compared. All images are single sections.

by an amide bond (DC8/1). Although ester-linked conjugates showed similar potency, when their effects were compared to dextrin content of the conjugate, they caused less apoptosis than the amide-linked conjugates. Varache et al<sup>44</sup> have previously demonstrated that increasing the degree of dextrin succinylation typically leads to a greater number of linkers bound to colistin, corresponding to the conjugate's antimicrobial activity. Even after degradation by amylase, residual linker groups, with differing lengths of glucose units attached, prevent complete restoration of colistin activity.

Compared to the amide-linked dextrin–colistin conjugates, colistin sulfate and ester-linked dextrin–colistin conjugates induced less annexin V binding and caspase 3/7 dependent cell death. This suggests that the residual linker groups remaining attached to colistin may play a key role in the activation of caspase 3/7 apoptosis.<sup>30</sup> Conjugation efficiency of ester-linked conjugates was generally lower than those containing amide linkers, meaning that conjugates contained more unreacted dextrin. The presence of free dextrin in polymer conjugates has been previously reported.<sup>14</sup> Removal of unreacted dextrin using size-exclusion chromatography is challenging, since its size is relatively similar to the dextrin–colistin conjugate. At the concentrations used for antibacterial activity (typically 2–16  $\mu$ g colistin base/mL), the



succinoylated dextrin concentration contained in the conjugates is not toxic. However, to achieve the high concentrations of colistin required to cause cell death in leukemia cell lines, the dextrin content of conjugates exceeded safe levels and masked the effects of colistin.

The mechanism of polymyxin nephrotoxicity has been widely studied and is related to colistin's interaction with oxidative stress and death-related pathways such as necrosis, apoptosis and autophagy.<sup>45</sup> Here, necrosis, but not apoptosis, was the main mode of cell death by colistin sulfate in both kidney and leukemia cell lines. However, DC8/1 caused caspase-dependent apoptosis in leukemia cells, suggesting that this chemical modification of colistin alters the mechanism of cell death. Induction of annexin V binding, and thus apoptosis, occurred within a few hours of exposure to DC8/1, and cell death was extensive by 24 h, suggesting that the mechanism of cytotoxicity may not be mediated through induction of differentiation, for example, by LSD1 inhibition. Preliminary studies found no evidence of upregulation of CD11b or CD86 following 48 h treatment with DC8/1 and 24 h recovery (data not shown).

Whilst at higher concentrations, some of the dextrin–colistin conjugates caused an apparent increase in DNA content, subsequent analysis did not show any cell cycle disruption. As a characterized efflux pump substrate (eg ATP-binding cassette (ABC) transporter proteins), we propose that the increased Hoechst 33342 uptake, which was greatest for dextrin–colistin conjugates containing 10 mol% succinoylated dextrin, may be due to altered activity or expression of these proteins in the leukemia cell lines, rather than G2 cell cycle accumulation. Cell cycle disruption has been linked to LSD1/KDM1A inhibition, for example, Nicosia et al<sup>46</sup> demonstrated cell cycle inhibition, via downregulation of a LSD1/KDM1A target in the acute promyelocytic leukemia cell line, NB-4. Interestingly, although none of the colistin treatments tested here altered the cell cycle in leukemia cells, Dai et al<sup>45</sup> did observe cell cycle arrest in a murine nephrotoxicity model and Eadon et al found that homogenized kidney tissue of mice who were administered colistin had altered expression of genes that regulate the cell cycle,<sup>47</sup> which suggests a tissue-specific effect. Reduced colony-forming ability of leukemia cell lines correlated with cell viability at 24 h, suggesting that colony forming cells were not preferentially targeted by either colistin sulfate or the dextrin–colistin conjugates.

Here, we were unable to establish the exact mechanism of enhanced cytotoxicity of DC8/1, and we did not observe any evidence of LSD1/KDM1A inhibition. However, Smitheman<sup>48</sup> observed peak LSD1/KDM1A inhibition of leukemia cell lines (including MV-4-11 and THP-1) treated with sub-lethal concentrations of LSD1/KDM1A inhibitors (GSK2879552 and GSK-LSD1) at 3–6 days, with no evidence of apoptosis. Colony formation results suggested that the main impact on the functionality of surviving cells occurred within 24 h of treatment, which supports the timescales used in our cytotoxicity experiments.

## Clinical Potential of Dextrin–Colistin Conjugates to Treat AML

Drug repurposing (also known as drug repositioning, reprofiling or re-tasking) is a process of identifying new uses for existing drugs beyond the scope of the original medical indication.<sup>49</sup> The advantages of this approach include lower risk of failure, shorter time to market and reduced drug development costs.<sup>50</sup> Recently, several antibiotics have been repurposed to treat cancer.<sup>51</sup> For example, levofloxacin was shown to inhibit proliferation and induce apoptosis of lung cancer cells in preclinical studies<sup>52</sup> and doxycycline has shown anti-proliferative and pro-apoptotic activity in cervical cancer and breast cancer cell lines.<sup>53,54</sup> Of the 371 drugs currently being evaluated in clinical trials as potential treatments for various cancers, 10 are antibiotics.<sup>55</sup> Nevertheless, antibiotic repurposing remains controversial, due to the potential impact on the development of antimicrobial resistance (AMR),<sup>56</sup> which correlates strongly with increased consumption.<sup>57,58</sup> AML is an aggressive condition that requires rapid and effective treatment that can last for several years. Prolonged antibiotic use may induce drug resistance among gut microbes or create antibiotic resistance that could reduce the effectiveness of treatments for common infections or render the patients more prone to infection.

When intravenous colistin (usually administered as the prodrug, colistimethate sodium (CMS)) is used to treat patients with Gram-negative bacterial infections, a target average colistin plasma concentration at steady-state ( $C_{ss,avg}$ ) of 2 mg/L is usually used,<sup>59</sup> corresponding to the minimum inhibitory concentration clinical breakpoint for several Gram-negative pathogens. However, at plasma colistin concentrations of >2.5 mg/L, the risk of concentration-dependent nephrotoxicity increases substantially.<sup>60,61</sup> In agreement with previous studies,<sup>11</sup> dextrin–colistin conjugates were ~3-fold less toxic to the kidney cell line. While this is a key development in tackling the cytotoxicity of colistin to



normal tissues, ultimately, it is probably unfeasible that the  $IC_{50}$  values seen for colistin and dextrin–colistin conjugates in leukemia cell lines (exceeding 235 mg/L) could be achieved clinically without causing severe nephrotoxicity. Although therapeutic concentrations of dextrin–colistin conjugate are unlikely to be achieved clinically, this approach could be applied to modify other, more potent, non-antibiotic therapeutics that have shown promise for the treatment of AML to reduce toxic side effects and boost potency.

## Conclusion

This study has demonstrated the potentiation of colistin's anti-leukemic activity by covalent, irreversible attachment of dextrin, which was unlikely to be dependent on LSD1/KDM1A. Our results show that, despite cellular uptake being effectively reduced by dextrin attachment, polymer conjugation can enhance the biological activity of a drug, alter its mechanism of action and localize drugs to endolysosomes. Whilst clinical translation of dextrin–colistin conjugates for the treatment of AML is unlikely due to the potential to promote AMR and the relatively high colistin concentrations required for anticancer activity *in vivo*, the ability to potentiate the effectiveness of an anticancer drug by polymer conjugation, while reducing side effects and improving biodistribution of the drug, is very attractive, and this approach warrants further investigation. The future design of polymer conjugates bearing alternative LSD1/KDM1A inhibitors should consider incorporating specific ligands or antibodies to enhance endocytosis and organelle targeting. Future studies should also include toxicity testing in CD34+ cells from healthy human donors.

## Data Sharing Statement

Information on the data underpinning the results presented here, including how to access them, can be found in the Cardiff University data catalogue at <http://doi.org/10.17035/d.2024.0322456854>.

## Acknowledgments

This article is dedicated to the memory of Dr Konrad Beck, who presented the idea of investigating dextrin–colistin conjugates as an LSD1 inhibitor to treat cancer. The authors acknowledge Miss Gilda Pourbahram and Miss Amanda Gilbert for their contributions to literature review and method development, respectively. We also acknowledge the technical cell culture support provided by Dr Sarah Youde and Dr Maria Stack and thank Dr Catherine Naseriyan from Central Biotechnology Services, Cardiff University for her technical expertise in FACS. This paper has been uploaded to bioRxiv as a preprint: <https://www.biorxiv.org/content/10.1101/2023.11.09.565276v1>.

## Author Contributions

All authors made a significant contribution to the work reported, whether that is in the conception, study design, execution, acquisition of data, analysis and interpretation, or in all these areas; took part in drafting, revising or critically reviewing the article; gave final approval of the version to be published; have agreed on the journal to which the article has been submitted; and agree to be accountable for all aspects of the work.

## Funding

This research was funded in whole, or in part, by the Wellcome Trust (204824/Z/16/Z). This research was also funded by Cardiff University and UK Medical Research Council (MR/N023633/1). For the purpose of open access, the author has applied a CC BY public copyright license to any Author Accepted Manuscript version arising from this submission. The funders had no role in the design of the study; in the collection, analyses, or interpretation of data; in the writing of the manuscript, or in the decision to publish the results.

## Disclosure

Dr Siân Rizzo's current affiliation is at Department of Haematology, School of Medicine, Cardiff University, Cardiff, UK. Dr Mathieu Varache's current affiliation is at Advanced BioDesign, 655 All. des Parcs, 69800 Saint-Priest, France. Dr Elaine Ferguson and Prof David Thomas report a patent EP2585114B1 issued. The authors report no other conflicts of interest in this work.

## References

1. Bowman RL, Busque L, Levine RL. Clonal hematopoiesis and evolution to hematopoietic malignancies. *Cell Stem Cell*. 2018;22(2):157–170. doi:10.1016/j.stem.2018.01.011
2. Papaemmanuil E, Gerstung M, Bullinger L, et al. Genomic classification and prognosis in acute myeloid leukemia. *N Engl J Med*. 2016;374(23):2209–2221. doi:10.1056/NEJMoa1516192
3. UK CR. Acute myeloid leukaemia (AML) statistics. Cancer Research UK; 2020. <https://www.cancerresearchuk.org/health-professional/cancer-statistics/statistics-by-cancer-type/leukaemia-aml>. Accessed June, 2022.
4. Ito T, Sanford D, Tomuleasa C, et al. Healthcare resource utilization trends in patients with acute myeloid leukemia ineligible for intensive chemotherapy receiving first-line systemic treatment or best supportive care: a multicenter international study. *Eur J Haematol*. 2022;109(1):58–68. doi:10.1111/ejh.13769
5. Heo YA, Syed YY, Keam SJ. Pegaspargase: a review in acute lymphoblastic leukaemia. *Drugs*. 2019;79(7):767–777. doi:10.1007/s40265-019-01120-1
6. Tzogani K, Penttila K, Lapvetelainen T, et al. EMA review of daunorubicin and cytarabine encapsulated in liposomes (Vyxeos, CPX-351) for the treatment of adults with newly diagnosed, therapy-related acute myeloid leukemia or acute myeloid leukemia with myelodysplasia-related changes. *Oncologist*. 2020;25(9):e1414–e1420. doi:10.1634/theoncologist.2019-0785
7. Floc'h N, Ashton S, Taylor P, et al. Optimizing therapeutic effect of aurora B inhibition in acute myeloid leukemia with AZD2811 Nanoparticles. *Mol Cancer Ther*. 2017;16(6):1031–1040. doi:10.1158/1535-7163.MCT-16-0580
8. Zhang R, Yang J, Zhou Y, Shami PJ, Kopecek J. N-(2-Hydroxypropyl)methacrylamide copolymer-drug conjugates for combination chemotherapy of acute myeloid leukemia. *Macromol Biosci*. 2016;16(1):121–128. doi:10.1002/mabi.201500193
9. Ferguson EL, Duncan R. Dextrin-phospholipase A2: synthesis and evaluation as a bioresponsive anticancer conjugate. *Biomacromolecules*. 2009;10(6):1358–1364. doi:10.1021/bm8013022
10. Hardwicke J, Ferguson EL, Moseley R, Stephens P, Thomas DW, Duncan R. Dextrin-rhEGF conjugates as bioresponsive nanomedicines for wound repair. *J Control Release*. 2008;130(3):275–283. doi:10.1016/j.jconrel.2008.07.023
11. Ferguson EL, Azzopardi E, Roberts JL, Walsh TR, Thomas DW. Dextrin-colistin conjugates as a model bioresponsive treatment for multidrug resistant bacterial infections. *Mol Pharm*. 2014;11(12):4437–4447. doi:10.1021/mp500584u
12. Hreczuk-Hirst D, Chicco D, German L, Duncan R. Dextrins as potential carriers for drug targeting: tailored rates of dextrin degradation by introduction of pendant groups. *Int J Pharm*. 2001;230(1–2):57–66. doi:10.1016/S0378-5173(01)00859-6
13. Hreczuk-Hirst D, German L, Duncan R. Dextrins as carriers for drug targeting: reproducible succinylation as a means to introduce pendant groups. *J Bioact Compat Polym*. 2001;16(5):353–365. doi:10.1106/QBKY-E3VM-19K4-3GA5
14. Duncan R, Gilbert HRP, Carbajo RJ, Vicent MJ. Polymer Masked-Unmasked Protein Therapy (PUMPT) 1. Bioresponsive dextrin-trypsin and -MSH conjugates designed for  $\alpha$ -amylase activation. *Biomacromolecules*. 2008;9(4):1146–1154. doi:10.1021/bm701073n
15. Zhang L, Zhao Y, Ding W, et al. Autophagy regulates colistin-induced apoptosis in PC-12 cells. *Antimicrob Agents Chemother*. 2015;59(4):2189–2197. doi:10.1128/AAC.04092-14
16. Verstovsek S, Maccubbin DL, Ehrke MJ, Mihich E. Polymyxin B-mediated lysis of tumor cells. *Int Arch Allergy Immunol*. 1993;100(1):47–52. doi:10.1159/000236386
17. Speranzini V, Rotili D, Ciossani G, et al. Polymyxins and quinazolines are LSD1/KDM1A inhibitors with unusual structural features. *Sci Adv*. 2016;2(9):e1601017. doi:10.1126/sciadv.1601017
18. Schenk T, Chen WC, Gollner S, et al. Inhibition of the LSD1 (KDM1A) demethylase reactivates the all-trans-retinoic acid differentiation pathway in acute myeloid leukemia. *Nat Med*. 2012;18(4):605–611. doi:10.1038/nm.2661
19. Fang Y, Liao G, Yu B. LSD1/KDM1A inhibitors in clinical trials: advances and prospects. *J Hematol Oncol*. 2019;12(1):129. doi:10.1186/s13045-019-0811-9
20. Wass M, Gollner S, Besenbeck B, et al. A proof of concept Phase I/II pilot trial of LSD1 inhibition by tranlycypromine combined with ATRA in refractory/relapsed AML patients not eligible for intensive therapy. *Leukemia*. 2021;35(3):701–711. doi:10.1038/s41375-020-0892-z
21. Pohlen M, Marx J, Mellmann A, et al. Ciprofloxacin versus colistin prophylaxis during neutropenia in acute myeloid leukemia: two parallel patient cohorts treated in a single center. *Haematologica*. 2016;101(10):1208–1215. doi:10.3324/haematol.2016.147934
22. Eljaaly K, Bidell MR, Gandhi RG, et al. Colistin nephrotoxicity: meta-analysis of randomized controlled trials. *Open Forum Infect Dis*. 2021;8(2):ofab026. doi:10.1093/ofid/ofab026
23. Azzopardi EA, Ferguson EL, Thomas DW. Development and validation of an in vitro pharmacokinetic/pharmacodynamic model to test the antibacterial efficacy of antibiotic polymer conjugates. *Antimicrob Agents Chemother*. 2015;59(4):1837–1843. doi:10.1128/AAC.03708-14
24. Roberts JL, Cattoz B, Schweins R, et al. In vitro evaluation of the interaction of dextrin-colistin conjugates with bacterial lipopolysaccharide. *J Med Chem*. 2016;59(2):647–654. doi:10.1021/acs.jmedchem.5b01521
25. Varache M, Rizzo S, Sayers EJ, et al. Dextrin conjugation to colistin inhibits its toxicity, cellular uptake and acute kidney injury in vivo. *bioRxiv*. 2023;11565265.
26. Duncan R. Designing polymer conjugates as lysosomotropic nanomedicines. *Biochem Soc Trans*. 2007;35(Pt 1):56–60. doi:10.1042/BST0350056
27. Haag R, Kratz F. Polymer therapeutics: concepts and applications. *Angew Chem*. 2006;45(8):1198–1215. doi:10.1002/anie.200502113
28. Brown MD, Schatzlein AG, Uchegbu IF. Gene delivery with synthetic (non viral) carriers. *Int J Pharm*. 2001;229(1–2):1–21. doi:10.1016/S0378-5173(01)00861-4
29. Ferguson EL, Richardson SC, Duncan R. Studies on the mechanism of action of dextrin-phospholipase A2 and its suitability for use in combination therapy. *Mol Pharm*. 2010;7(2):510–521. doi:10.1021/mp900232a
30. Stokniene J, Powell LC, Aarstad OA, et al. Bi-functional alginate oligosaccharide-polymyxin conjugates for improved treatment of multidrug-resistant gram-negative bacterial infections. *Pharmaceutics*. 2020;12(11):1080. doi:10.3390/pharmaceutics12111080
31. Richardson SC, Wallom KL, Ferguson EL, et al. The use of fluorescence microscopy to define polymer localisation to the late endocytic compartments in cells that are targets for drug delivery. *J Control Release*. 2008;127(1):1–11. doi:10.1016/j.jconrel.2007.12.015
32. Ryan MJ, Johnson G, Kirk J, Fuerstenberg SM, Zager RA, Torok-Storb B. HK-2: an immortalized proximal tubule epithelial cell line from normal adult human kidney. *Kidney Int*. 1994;45(1):48–57. doi:10.1038/ki.1994.6

33. Wu Y, Connors D, Barber L, Jayachandra S, Hanumegowda UM, Adams SP. Multiplexed assay panel of cytotoxicity in HK-2 cells for detection of renal proximal tubule injury potential of compounds. *Toxicol In Vitro*. 2009;23(6):1170–1178. doi:10.1016/j.tiv.2009.06.003
34. Ormerod M. DNA Analysis. In: Ormerod M, editor. *Flow Cytometry. A Practical Approach*. 3 ed. Oxford, UK: Oxford University Press; 2000:83–90.
35. Watson JV, Chambers SH, Smith PJ. A pragmatic approach to the analysis of DNA histograms with a definable G1 peak. *Cytometry*. 1987;8(1):1–8. doi:10.1002/cyto.990080101
36. Schindelin J, Arganda-Carreras I, Frise E, et al. Fiji: an open-source platform for biological-image analysis. *Nat Methods*. 2012;9(7):676–682. doi:10.1038/nmeth.2019
37. Bedard PL, Hyman DM, Davids MS, Siu LL. Small molecules, big impact: 20 years of targeted therapy in oncology. *Lancet*. 2020;395(10229):1078–1088. doi:10.1016/S0140-6736(20)30164-1
38. Cucchi DGJ, Polak TB, Ossenkoppele GJ, et al. Two decades of targeted therapies in acute myeloid leukemia. *Leukemia*. 2021;35(3):651–660. doi:10.1038/s41375-021-01164-x
39. Manzari MT, Shamay Y, Kiguchi H, Rosen N, Scaltriti M, Heller DA. Targeted drug delivery strategies for precision medicines. *Nat Rev Mater*. 2021;6(4):351–370. doi:10.1038/s41578-020-00269-6
40. Zhang S, Liu M, Yao Y, Yu B, Liu H. Targeting LSD1 for acute myeloid leukemia (AML) treatment. *Pharmacol Res*. 2021;164:105335. doi:10.1016/j.phrs.2020.105335
41. Fioravanti R, Romanelli A, Mautone N, et al. Tranylcyproline-based LSD1 inhibitors: structure-activity relationships, antiproliferative effects in leukemia, and gene target modulation. *ChemMedChem*. 2020;15(7):643–658. doi:10.1002/cmde.201900730
42. Rosenzweig J, Coutinho DF, Long M, et al. Effects of LSD1 inhibition with img-7289 on the leukemia initiating cell population with induction of differentiation and cell death in pediatric relapsed/refractory AML. *Blood*. 2022;140(Supplement 1):5944–5945. doi:10.1182/blood-2022-165408
43. Barretina J, Caponigro G, Stransky N, et al. The Cancer Cell Line Encyclopedia enables predictive modelling of anticancer drug sensitivity. *Nature*. 2012;492(7428):290. doi:10.1038/nature11735
44. Varache M, Powell LC, Aarstad OA, et al. Polymer masked-unmasked protein therapy: identification of the active species after amylase activation of dextrin-colistin conjugates. *Mol Pharm*. 2019;16(7):3199–3207. doi:10.1021/acs.molpharmaceut.9b00393
45. Dai C, Li J, Tang S, Li J, Xiao X. Colistin-induced nephrotoxicity in mice involves the mitochondrial, death receptor, and endoplasmic reticulum pathways. *Antimicrob Agents Chemother*. 2014;58(7):4075–4085. doi:10.1128/AAC.00070-14
46. Nicosia L, Boffo FL, Ceccacci E, et al. Pharmacological inhibition of LSD1 triggers myeloid differentiation by targeting GSE1 oncogenic functions in AML. *Oncogene*. 2022;41(6):878–894. doi:10.1038/s41388-021-02123-7
47. Eadon MT, Hack BK, Alexander JJ, Xu C, Dolan ME, Cunningham PN. Cell cycle arrest in a model of colistin nephrotoxicity. *Physiol Genomics*. 2013;45(19):877–888. doi:10.1152/physiolgenomics.00076.2013
48. Smitheman KN, Severson TM, Rajapurkar SR, et al. Lysine specific demethylase 1 inactivation enhances differentiation and promotes cytotoxic response when combined with all-trans retinoic acid in acute myeloid leukemia across subtypes. *Haematologica*. 2019;104(6):1156–1167. doi:10.3324/haematol.2018.199190
49. Ashburn TT, Thor KB. Drug repositioning: identifying and developing new uses for existing drugs. *Nat Rev Drug Discov*. 2004;3(8):673–683. doi:10.1038/nrd1468
50. Pushpakom S, Iorio F, Eyers PA, et al. Drug repurposing: progress, challenges and recommendations. *Nat Rev Drug Discov*. 2019;18(1):41–58. doi:10.1038/nrd.2018.168
51. Pfab C, Schnobrich L, Eldnasoury S, Gessner A, El-Najjar N. Repurposing of antimicrobial agents for cancer therapy: what do we know? *Cancers*. 2021;13(13):3193. doi:10.3390/cancers13133193
52. Song M, Wu H, Wu S, et al. Antibiotic drug levofloxacin inhibits proliferation and induces apoptosis of lung cancer cells through inducing mitochondrial dysfunction and oxidative damage. *Biomed Pharmacother*. 2016;84:1137–1143. doi:10.1016/j.biopha.2016.10.034
53. Zhao Y, Wang X, Li L, Li C. Doxycycline inhibits proliferation and induces apoptosis of both human papillomavirus positive and negative cervical cancer cell lines. *Can J Physiol Pharmacol*. 2016;94(5):526–533. doi:10.1139/cjpp-2015-0481
54. Zhang L, Xu L, Zhang F, Vlashi E. Doxycycline inhibits the cancer stem cell phenotype and epithelial-to-mesenchymal transition in breast cancer. *Cell Cycle*. 2017;16(8):737–745. doi:10.1080/15384101.2016.1241929
55. Pantziarka P, Verbaanderd C, Sukhatme V, et al. ReDO\_DB: the repurposing drugs in oncology database. *Ecancermedicalscience*. 2018;12:886. doi:10.3332/ecancer.2018.886
56. Talat A, Bashir Y, Khan AU. Repurposing of Antibiotics: sense or Non-sense. *Front Pharmacol*. 2022;13:833005. doi:10.3389/fphar.2022.833005
57. Mladenovic-Antic S, Kocic B, Velickovic-Radovanovic R, et al. Correlation between antimicrobial consumption and antimicrobial resistance of *Pseudomonas aeruginosa* in a hospital setting: a 10-year study. *J Clin Pharm Ther*. 2016;41(5):532–537. doi:10.1111/jcpt.12432
58. Liang C, Zhang X, Zhou L, Meng G, Zhong L, Peng P. Trends and correlation between antibacterial consumption and carbapenem resistance in gram-negative bacteria in a tertiary hospital in China from 2012 to 2019. *BMC Infect Dis*. 2021;21(1):444. doi:10.1186/s12879-021-06140-5
59. Nation RL, Rigatto MHP, Falci DR, Zavascki AP. Polymyxin acute kidney injury: dosing and other strategies to reduce toxicity. *Antibiotics*. 2019;8(1):24. doi:10.3390/antibiotics8010024
60. Horcajada JP, Sorli L, Luque S, et al. Validation of a colistin plasma concentration breakpoint as a predictor of nephrotoxicity in patients treated with colistin methanesulfonate. *Int J Antimicrob Agents*. 2016;48(6):725–727. doi:10.1016/j.ijantimicag.2016.08.020
61. Forrest A, Garonzik SM, Thamlikitkul V, et al. Pharmacokinetic/toxicodynamic analysis of colistin-associated acute kidney injury in critically ill patients. *Antimicrob Agents Chemother*. 2017;61(11). doi:10.1128/AAC.01367-17

International Journal of Nanomedicine

Dovepress

### Publish your work in this journal

The International Journal of Nanomedicine is an international, peer-reviewed journal focusing on the application of nanotechnology in diagnostics, therapeutics, and drug delivery systems throughout the biomedical field. This journal is indexed on PubMed Central, MedLine, CAS, SciSearch<sup>®</sup>, Current Contents<sup>®</sup>/Clinical Medicine, Journal Citation Reports/Science Edition, EMBase, Scopus and the Elsevier Bibliographic databases. The manuscript management system is completely online and includes a very quick and fair peer-review system, which is all easy to use. Visit <http://www.dovepress.com/testimonials.php> to read real quotes from published authors.

Submit your manuscript here: <https://www.dovepress.com/international-journal-of-nanomedicine-journal>